第 35 卷第 10 期
2019 年 10 月

无 机 化 学 学 报
CHINESE JOURNAL OF INORGANIC CHEMISTRY

Vol.35 No.10
1805-1812

两个基于$[SMo_{12}O_{40}]^{2-}$和冠醚基超分子阳离子的无机–有机杂化晶体的合成及晶体结构

熊 俊[1] 谭茂坤[1] 吕少仿[1] 李 明*,[1] 杨水彬*,[2]

([1]武汉纺织大学化学与化工学院,湖北省生物质纤维与生态染整重点实验室,武汉 430200)

([2]黄冈师范学院化工学院,催化材料制备及应用湖北省重点实验室,黄冈 438000)

摘要:以 18-冠-6 和 4-碘–苯铵盐,二苯并 30-冠-10 和 3-氟-4-氯–苯铵盐为超分子阳离子构建单元,分别引入到 Keggin 型$[SMo_{12}O_{40}]^{2-}$中,使用 H 管扩散法和溶剂挥发法合成了无机–有机杂化材料$[(4\text{-I-Anis})([18]\text{crown-6})]_2[SMo_{12}O_{40}]\cdot CH_3CN$ (**1**)和$[(3\text{-F-4-Cl-Anis})_2(DB[30]\text{crown-10})][SMo_{12}O_{40}]\cdot 2CH_3CN$ (**2**)(4-I-Anis=4-碘–苯铵盐;3-F-4-Cl-Anis=3-氟-4-甲基苯铵盐;DB[30]crown-10=二苯并 30-冠-10)。通过红外光谱、元素分析、热重分析、固态漫反射光谱和 X 射线单晶结构分析对化合物进行了表征。结构分析表明,晶体 **1** 和 **2** 通过非共价键自组装作用构建而成,冠醚基超分子阳离子是通过 N–H···O 氢键作用形成。晶体 **1** 中,在 *bc* 平面,每个$[SMo_{12}O_{40}]^{2-}$多酸阴离子被 6 个超分子阳离子(4-I-Anis)([18]crown-6)围绕,形成六边形的结构;晶体 **2** 中,在 *bc* 平面,每个$[SMo_{12}O_{40}]^{2-}$多酸阴离子被 4 个大的超分子阳离子$(3\text{-F-4-Cl-Anis})_2(DB[30]\text{crown-10})$围绕,形成四边形的结构。热重分析表明,氢键在维持晶体 **1** 和 **2** 的稳定性上起着主要的作用。固态漫反射光谱表明,$[SMo_{12}O_{40}]^{2-}$和冠醚基超分子阳离子之间存在电荷转移作用。

关键词:无机–有机杂化物;超分子自组装;多金属氧酸盐;冠醚;超分子阳离子

中图分类号:O614.61+2 **文献标识码**:A **文章编号**:1001-4861(2019)10-1805-08

DOI:10.11862/CJIC.2019.208

Two Inorganic-Organic Hybrid Crystals Based on $[SMo_{12}O_{40}]^{2-}$ Polyoxometallates and Supramolecular Cation: Syntheses and Crystal Structures

XIONG Jun[1] TAN Mao-Kun[1] LÜ Shao-Fang[1] LI Ming*,[1] YANG Shui-Bin*,[2]

([1]*Hubei Key Laboratory of Biomass Fibers and Eco-dyeing & Finishing, College of Chemistry and Chemical Engineering, Wuhan Textile University, Wuhan* 430200, *China*)

([2]*Hubei Key Laboratory for Processing and Application of Catalytic Materials, College of Chemical Engineering, Huanggang Normal University, Huanggang, Hubei* 438000, *China*)

Abstract: Two inorganic-organic hybrids, $[(4\text{-I-Anis})([18]\text{crown-6})]_2[SMo_{12}O_{40}]\cdot CH_3CN$ (**1**) and $[(3\text{-F-4-Cl-Anis})_2(DB[30]\text{crown-10})][SMo_{12}O_{40}]\cdot 2CH_3CN$ (**2**) (4-I-Anis=4-iodoanilinium; 3-F-4-Cl-Anis=3-fluoro-4-chloroanilinium; DB[30]crown-10=dibenzo[30]crown-10) have been synthesized and characterized by infrared spectrum (IR), elemental analysis (EA), powder XRD, thermogravimetric (TG), solid state diffuse reflectance spectra (DRS) and X-ray diffraction. Crystals **1** and **2** are constructed through noncovalent bonding interaction, and the polyoxometalates and supramolecular cation arrange alternately. Supramolecular cation forms through the N–H ··· O hydrogen bonding interaction between the nitrogen atom of anilinium and oxygen atoms of crown ether derivatives. In crystal **1**, each polyoxoanion is surrounded by six monovalent supramolecular cations (4-I-Anis)([18]crown-6) and forms hexagonal arrangement in *bc* plane. In crystal **2**, each polyoxoanion is surrounded by four

收稿日期:2019-03-04。收修改稿日期:2019-07-29。

湖北省自然自然科学基金(No.2018CFB402),武汉纺织大学未来之星助推计划(No.165002)和催化材料制备及应用湖北省重点实验室开放基金(No.201829203)资助项目。

*通信联系人。E-mail:lim@wtu.edu.cn,2416975012@qq.com

large supramolecular cations $(3\text{-F-4-Cl-Anis})_2$(DB[30]crown-10) and forms tetragonal arrangement in *bc* plane. TG measurement indicated that hydrogen bonding interaction plays an important role in maintaining the structural stability of crystals **1** and **2**. DRS indicated that there exists charge-transfer interaction between $[SMo_{12}O_{40}]^{2-}$ polyoxoanions and crown ether based supramolecular cations in crystals **1** and **2**. CCDC: 1540103, **1**; 1899810, **2**.

Keywords: inorganic–organic hybrids; supramolecular self–assembled; polyoxometallates; crown ether; supramolecular cation

Over the past several decades, inorganic-organic hybrid materials have intrigued people′s interest because of their fantastic architecture and interesting chemical properties[1-4]. Crystalline structures designed via noncovalent bonding interaction are one of the indispensable part in the inorganic-organic hybrid field[5-6]. Polyoxometalates (POMs) have attracted much attention in photochemistry, magnetic and catalytic fields due to their versatile architecture and unexpected properties[7-11]. POMs are discrete early transition metal-oxide cluster anions and comprise a class of inorganic complexes, which are composed of several assembled $[MO_n]$ (M belongs to the *d*-block element in high oxidation state). As the inorganic building block, POMs have many merits for constructing supramolecular structures due to their structural characteristics, such as giant structure and multiple potential hydrogen bonding sites[12-13]. For example, ferrocenyl derivatives with carbon atom hydrogen bonding sites as the organic building unit could form inorganic-organic hybrids with the POMs through C–H⋯O hydrogen bonding interaction, and ferrocenyl derivatives are embedded into the large space formed by giant POMs[14].

Crown ethers as a kind of macrocyclic compounds are composed of hetero donor atoms such as O, N, S or Se. Because of the structural characteristics, like large ring structures and multiple hydrogen bonding sites, crown ethers can be treated as a kind of organic building blocks[15-16]. For example, crown ether with large cave can capture cations to form supramolecular cation with anilinium derivatives. In addition, the exposure C, N, and O atom of crown ether are the potential hydrogen bonding sites to form inorganic-organic hybrids with inorganic building blocks.

Recently, many of inorganic-organic hybrids based on POMs and crown ethers have been reported by Nakamura group. They have systemically researched the relationship between the size of crown ether based supramolecular cation and crystalline packing pattern[17]. They also studied the effect of Keggin POMs on the (3-flouoranilinium) rotor[18]. Herein, we have synthesized two novel inorganic-organic hybrid, $[(4\text{-I-Anis})([18]\text{crown-6})]_2[SMo_{12}O_{40}]\cdot CH_3CN$ (**1**) and $[(3\text{-F-4-Cl-Anis})_2$ (DB [30]crown-10)$][SMo_{12}O_{40}]\cdot 2CH_3CN$ (**2**) (4-I-Anis =4-iodoanilinium; 3-F-4-Cl-Anis =3-fluoro-4-chloroanilinium; DB[30]crown-10=dibenzo[30]crown-10, Scheme 1), and analyzed their crystalline structure through X-ray diffraction.

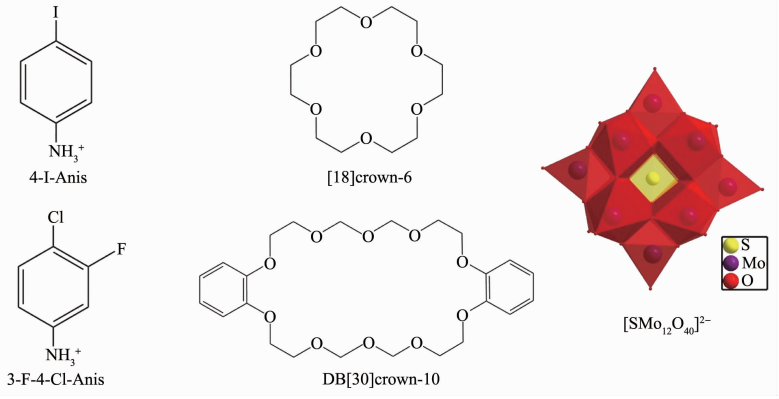

Scheme 1 Structures of 4-I-Anis, 3-F-4-Cl-Anis, [18]crown-6, DB[30]crown-10 and $[SMo_{12}O_{40}]^{2-}$

1 Experimental

1.1 Materials and measurements

[18]crown-6 and DB[30]crown-10, 4-iodoaniline and 4-chloro-3-fluoroaniline were purchased from Shanghai Aladdin Bio-Chem Technology Co., LTD, which were used without further purification. (4-I-Anis)(BF_4), (3-F-4-Cl-Anis)(BF_4) and $[TBA]_2[SMo_{12}O_{40}]$ were prepared according to similar procedures reported previously[15,19]. IR spectra were recorded using a Thermo Scientific Nicolet 6700 FT-IR spectrometer (400~7 800 cm^{-1}). Elemental analysis (C, H, N) was carried out on a CARLO ERBA 1106 analyzer. Powder XRD data of microcrystals were collected by using a Rigaku XtaLAB P200 diffractometer with graphite monochromated employing Cu $K\alpha$ radiation (λ=0.154 187 nm). The working voltage and current is 40 kV and 40 mA respectively, and the scanning range is from 3° to 40°. Solid state diffuse reflectance spectra of the samples were obtained for the dry pressed disk samples using a Shimazu UV-2550 spectrophotometer, equipped with an integrating sphere coated with polytetrafluoroethylene between 300 and 800 nm. TG curves were obtained on a Rigaku Thermoplus TG8120 thermal analysis station with Al_2O_3 reference. The temperature range was from 30 to 500 ℃ with a heating rate of 10 ℃·min^{-1} under flowing nitrogen gas.

1.2 Syntheses of [(4-I-Anis)([18]crown-6)]$_3$[$SMo_{12}O_{40}$]·CH_3CN (1) and [(3-F-4-Cl-Anis)$_2$(DB[30]crown-10)][$SMo_{12}O_{40}$]·$2CH_3CN$ (2)

Crystal **1** was synthesized using the standard diffusion method in an H-shape cell. Saturated CH_3CN solution (10 mL) of $[TBA]_2[SMo_{12}O_{40}]$ was added into the one side of H-shape cell. The acetonitrile solution (10 mL) containing (4-I-Anis)(BF_4) (20 mg, 0.10 mmol) and [18]crown-6 (26 mg, 0.10 mmol) were introduced into opposite sides of the H-shape cell. Then the cell was filled with acetonitrile slowly. After two week, the solution turned to black from green, which indicated that there existed charge transfer interaction. Black block crystals of **1** were obtained. Anal. Calcd. for $C_{38}H_{65}I_2Mo_{12}N_3O_{52}S$(%): C16.11, H 2.31, N 1.48; Found (%): C 16.13, H 2.27, N 1.50. IR (KBr pellet, cm^{-1}): 1 160(m), 1 060(m), 980(s), 870(m), 790(s).

Crystal **2** was synthesized using the evaporation method. (3-F-4-Cl-Anis)(BF_4) (0.40 mmol) and DB[30]crown-6 (0.20 mmol) dissolved in 10 mL acetonitrile was slowly added into saturated CH_3CN solution (10 mL) of $[TBA]_2[SMo_{12}O_{40}]$ with stirring. After one week, the solution turned to brown from green, which indicated that charge transfer interaction occurred, and black block crystals of **2** were obtained. Anal. Calcd. for $C_{44}H_{58}Cl_2F_2Mo_{12}N_4O_{50}S$ (%): C 19.32, H 2.12, N 2.05; Found (%): C 19.36, H 2.13, N 2.08. IR (KBr pellet, cm^{-1}): 1 170(m), 1 060(m), 970(s), 870(m), 780(s).

1.3 Crystal data and structure determination

Crystallographic data was collected using R-AXIS RAPID diffractometer with Mo $K\alpha$ radiation (λ= 0.071 073 nm) from a graphite monochromator at 173 K. The structures were solved by the direct method (SIR 2004) and expanded using Fourier transfer and refined on F^2 by the full-matrix least-squares method (SHELXL-97)[20-21]. All non-hydrogen atoms were refined using anisotropic temperature factors, and the hydrogen atoms were refined with theoretical calculated method using appropriate riding model. The crystallographic data of crystals **1** and **2** are summarized in Table 1.

CCDC: 1540103, **1**; 1899810, **2**.

Table 1　Crystallographic parameters for 1 and 2

Compound	1	2
Formula	$C_{38}H_{65}I_2Mo_{12}N_3O_{52}S$	$C_{44}H_{58}Cl_2F_2Mo_{12}N_4O_{50}S$
Formula weight	2 833.07	2 735.18
Size / mm	0.30×0.20×0.15	0.40×0.20×0.10
Crystal system	Triclinic	Triclinic
Space group	$P\bar{1}$	$P\bar{1}$
a / nm	1.184 5(2)	1.071 3(2)
b / nm	1.413 2(3)	1.209 2(2)

Continued Table 1

c / nm	2.562 4(5)	1.550 0(3)
α / (°)	101.20(3)	101.05(3)
β / (°)	96.04(3)	97.53(3)
γ / (°)	111.72(3)	96.12(3)
V / nm^3	3.834 4(17)	1.935 7(7)
Z	2	1
D_c / (g·cm^{-3})	2.454	2.346
μ / mm^{-1}	2.828	2.079
GOF on F^2	1.048	1.124
R_1[a] [$I>2\sigma(I)$]	0.046 8	0.034 1
wR_2[b] [$I>2\sigma(I)$]	0.125 3	0.095 0

[a] $R_1=\sum(|F_o|-|F_c|)/\sum|F_c|$; [b] $wR_2=[\sum w(F_o^2-F_c^2)^2/\sum w(F_o^2)^2]^{1/2}$

2 Results and disscussion

2.1 Structure description of crystal 1

Single crystal X-ray diffraction analysis reveals that the crystal **1** crystallizes in triclinic space group $P\bar{1}$. Crystal **1** contains two [18]crown-6 molecules, two 4-IAnis cations, one $[SMo_{12}O_{40}]^{2-}$ polyoxoanion and one CH_3CN molecule in the asymmetric unit as shown in Fig.1.

There are two kinds of supramolecular cations with different arrangements in crystal **1**. The supramolecular cations are constructed through the N-H···O hydrogen bonding interaction between the N atoms of 4-IAnis cations and the O atoms of [18] crown-6, and the N atoms are nearly located at the center of [18]crown-6 molecule. The average N–H···O hydrogen bonding lengths of N1-O (from O41 to O46) and N2-O (from O47 to O52) are 0.290 1 and 0.287 0 nm, respectively, which are similar to the standard N–H···O hydrogen bonding length[22], indicating there exist strong hydrogen bonding interactions between 4-IAnis cations and [18]crown-6 molecule. In the supramolecular cations, the 4-IAnis cationic plane containing N1 (or N2) is almost perpendicular to the [18]crown-6 molecular plane with the dihedral angle being 87.39° (or 89.56°).

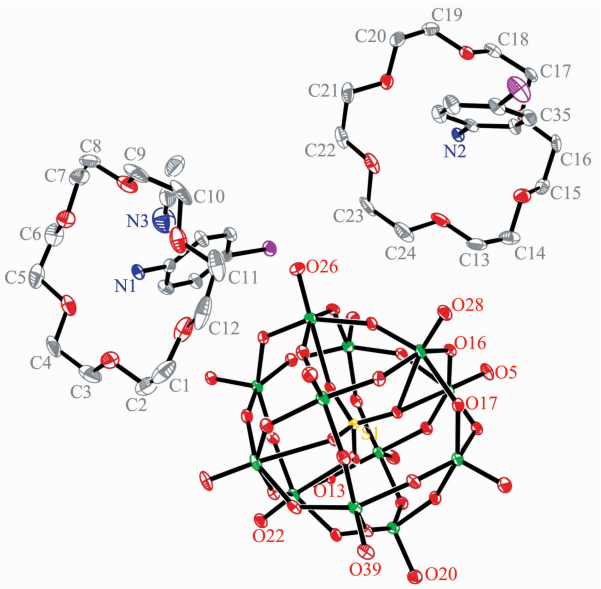

Hydrogen atoms are omitted, and only the atoms involved in the weak interaction are labeled for clarity

Fig.1 ORTEP diagram of asymmetric unit of crystal **1** with atomic numbering scheme and 30% thermal ellipsoids

$[SMo_{12}O_{40}]^{2-}$ polyoxoanion has an approximate O_h symmetry and consists of twelve sharing MoO_6 octahedrons. In crystal **1**, through X-ray crystalline structural analysis, short O ··· O distances between adjacent $[SMo_{12}O_{40}]^{2-}$ polyoxoanions were observed (O(5)···O(39) 0.328 9 nm; O(17)···O(28) 0.422 4 nm and O(22)···O(22) 0.316 8 nm), which indicates there exist intermolecular O···O interactions to construct a three-dimensional polyoxoanion structure. The clear polyoxoanion packing diagram is in *ac* plane as shown in Fig.2a. Weak hydrogen bonding interactions are found between $[SMo_{12}O_{40}]^{2-}$ polyoxoanions and [18] crown-6 molecule, which play an important role in constructing three-dimensional structure of **1**. The details of hydrogen bonding interactions are shown in Table 2. The divalent $[SMo_{12}O_{40}]^{2-}$ polyoxoanions and

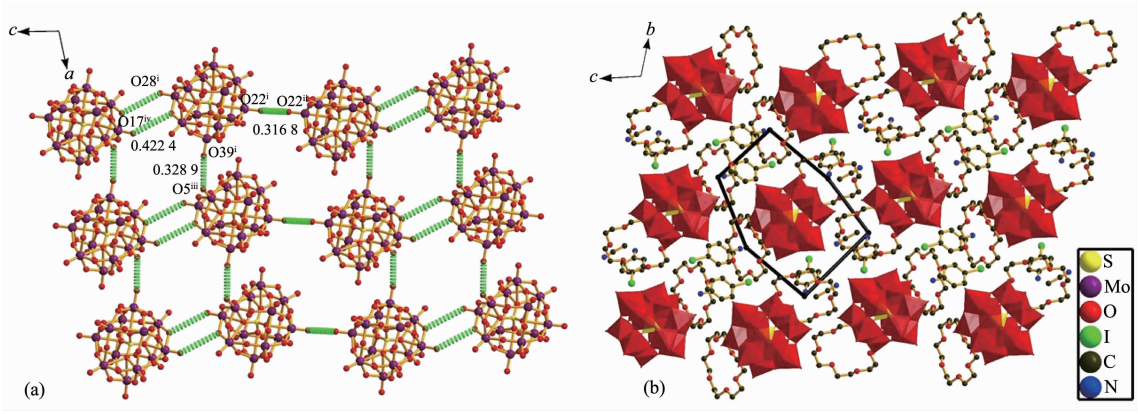

Symmetry codes: [i] $-2+x, y, z$; [ii] $-x, 2-y, -z$; [iii] $-1+x, y, z$; [iv] $-x, 2-y, 1-z$

Fig.2　(a) Packing diagram of $[SMo_{12}O_{40}]^{2-}$ polyoxoanions in crystal **1**; (b) Packing diagram of crystal **1** in *bc* plane

Table 2　Hydrogen bonding interaction parameters of crystal 1

D–H···A	*d*(D-H) / nm	*d*(H···A) / nm	*d*(D···A) / nm	∠DHA / (°)
C(6)–H(6B)···O(13)ⁱ	0.097(1)	0.256(1)	0.333 2(1)	137(3)
C(8)–H(8A)···O(31)ⁱⁱ	0.097(1)	0.255(1)	0.344 8(1)	155(3)
C(9)–H(9B)···O(39)ⁱⁱ	0.097(1)	0.249(1)	0.327 1(1)	138(3)
C(10)–H(10B)···O(5)ⁱⁱⁱ	0.097(1)	0.249(1)	0.341 5(1)	159(3)
C(11)–H(11B)···O(26)	0.097(1)	0.256(1)	0.352 9(2)	175(3)
C(13)–H(19A)···O(16)	0.097(1)	0.260(1)	0.353 6(1)	163(3)
C(22)–H(28A)···O(20)ⁱⁱ	0.097(1)	0.254(1)	0.345 3(1)	156(3)
C(35)–H(33)···O(5)ⁱᵛ	0.093(1)	0.258(1)	0.320 2(1)	125(3)

Symmetry codes: [i] $-1+x, y, z$; [ii] $x, -1+y, z$; [iii] $1-x, 1-y, -z$; [iv] $1-x, 2-y, 1-z$

monovalent [(4-IAnis)([18]crown-6)] assembly with the molar ratio of 1∶2. The supramolecular cations are filled into the space formed by $[SMo_{12}O_{40}]^{2-}$ polyoxoanions. Each $[SMo_{12}O_{40}]^{2-}$ polyoxoanions is surrounded by six [(4-IAnis)([18]crown-6)] supramolecular cations, and construct a hexagonal arrangement in *bc* plane as shown in Fig.2b.

2.2　Structure description of crystal 2

Single crystal X-ray diffraction analysis indicates that crystal **2** crystallizes in triclinic space group $P\bar{1}$. The asymmetric unit of crystal **2** contains half of a $[SMo_{12}O_{40}]^{2-}$ polyoxoanion, half of a DB[30]crown-10 molecule, one (3-F-4-Cl-Anis) cation and one CH_3CN molecule as shown in Fig.3. DB[30]crown-10 molecule has more larger cavity, which has the ability to incorporate two NH_4^+ cations. Therefore, in crystal **2**, supramolecular cations consisted of one DB[30]crown-10 molecule and two (3-F-4-Cl-Anis) cations. Each nitrogen atom in (3-F-4-Cl-Anis) cation is connected to five oxygen atoms in DB[30]crown-10 through N–H···O hydrogen bonding interaction with the same average N–H···O distance of 0.289 7 nm. Two aromatic planes of the (3-F-4-Cl-Anis) cations in the supramolecular cation are parallel to each other.

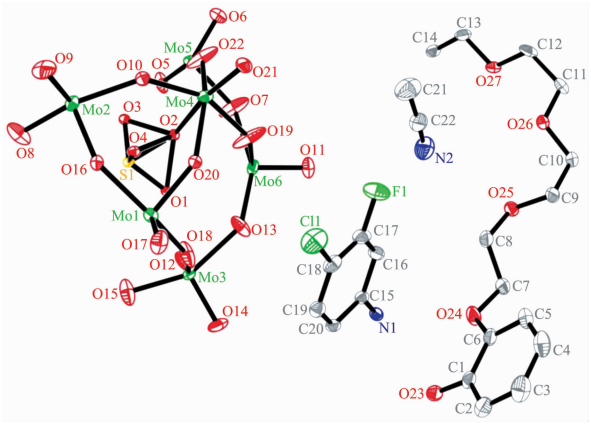

Hydrogen atoms are omitted for clarity

Fig.3　ORTEP diagram of asymmetric unit of crystal **2** with the atomic numbering scheme and 30% thermal ellipsoids

In crystal **2**, short O ⋯ O distances between adjacent $[SMo_{12}O_{40}]^{2-}$ polyoxoanions were found (O(9) ⋯O(21) 0.310 0 nm and O(7)⋯O(14) 0.322 2 nm), which indicates there exist intermolecular O ⋯ O interactions in *ab* plane as shown in Fig.4a. Weak hydrogen bonding interactions are observed between $[SMo_{12}O_{40}]^{2-}$ polyoxoanions and DB[30]crown-10 molecule, which play an important role in constructing three-dimensional structure of **2**. The details of hydrogen bonding interactions are shown in Table 3. The divalent $[SMo_{12}O_{40}]^{2-}$ polyoxoanions and divalent [(3-F-4-Cl-Anis)(DB [30]crown-10)] assembly with the molar ratio of 1∶1, and supramolecular cations are filled into the space formed by $[SMo_{12}O_{40}]^{2-}$ polyoxoanions. Each $[SMo_{12}O_{40}]^{2-}$ polyoxoanions is surrounded by four large size supramolecular cations [(3-F-4-Cl-Anis)(DB [30]crown-10)], and construct a rectangular arrangement in *bc* plane as shown in Fig.4b.

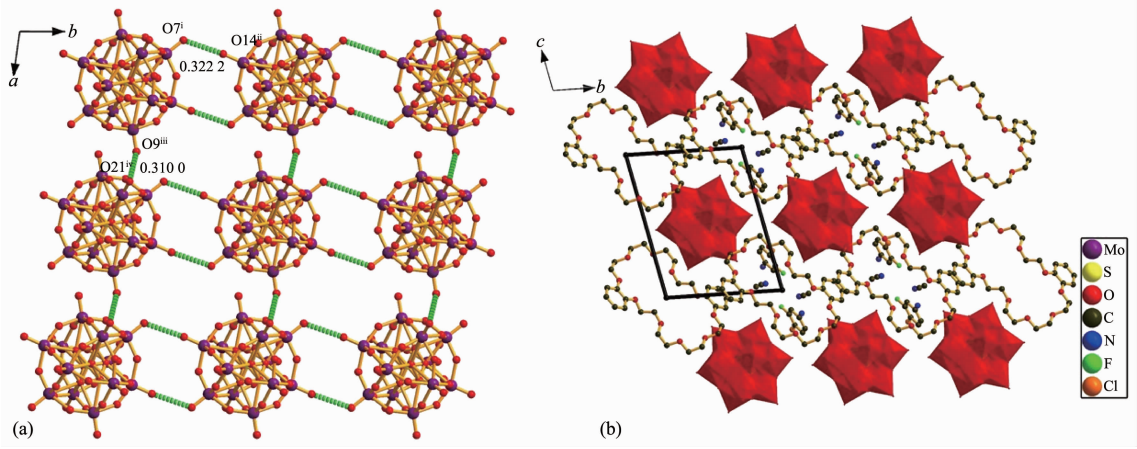

Symmetry codes: [i] −*x*, 1−*y*, 3−*z*; [ii] −1+*x*, *y*, 1+*z*; [iii] −1+*x*, −1+*y*, 1+*z*; [iv] 1−*x*, 1−*y*, 3−*z*

Fig.4 (a) Packing diagram of $[SMo_{12}O_{40}]^{2-}$ polyoxoanions in crystal **2**; (b) Packing diagram of crystal **2** in *bc* plane

Table 3 Hydrogen bonding interaction parameters of crystal 2

D–H⋯A	*d*(D-H) / nm	*d*(H⋯A) / nm	*d*(D⋯A) / nm	∠DHA / (°)
C(2)–H(2)⋯O(7)[i]	0.093(1)	0.253(1)	0.320 0(5)	129(2)
C(5)–H(5)⋯O(21)[ii]	0.093(1)	0.244(1)	0.320 6(7)	139(3)
C(7)–H(7A)⋯O(11)[iii]	0.097(1)	0.254(1)	0.343 4(7)	153(3)
C(20)–H(20)⋯O(27)[iii]	0.093(1)	0.256(1)	0.328 7(5)	136(3)
C(21)–H(21B)⋯O(6)[iv]	0.096(1)	0.259(1)	0.352 3(9)	164(3)

Symmetry codes: [i] −*x*, 1−*y*, 1−*z*; [ii] *x*, −1+*y*, *z*; [iii] 1−*x*, 1−*y*, 1−*z*; [iv] 1−*x*, 2−*y*, 1−*z*

2.3 XRD patterns of crystals 1 and 2

The powder X-ray patterns of crystals **1** and **2** were measured. As shown in Fig.5, the diffraction patterns of crystals **1** and **2** were very similar to the corresponding simulated PXRD pattern calculated from the crystalline structure. The results indicate that the phases of crystals **1** and **2** are pure.

2.4 Thermogravimetric analysis

The thermal behavior of crystals **1** and **2** was investigated through the TG-DTA measurements from 30 to 500 ℃ as shown in Fig.6. Crystal **1** started to decompose from 130 ℃. The weight loss of crystal **1** is mainly dominated by losing CH_3CN molecules during heating process. Crystal **1** lost one CH_3CN molecule (Obsd. 1.49%, Calcd. 1.45%) when the temperature is up to 152 ℃. Crystal **2** started to decompose from 160 ℃, and lost two CH_3CN molecules (Obsd. 3.00%, Calcd. 3.05%) when the temperature is up to 190 ℃. TG-DTA results are in accordance with the crystalline structure analysis, and indicate that the hydrogen bonding interaction plays an important role in maintaining the stability of

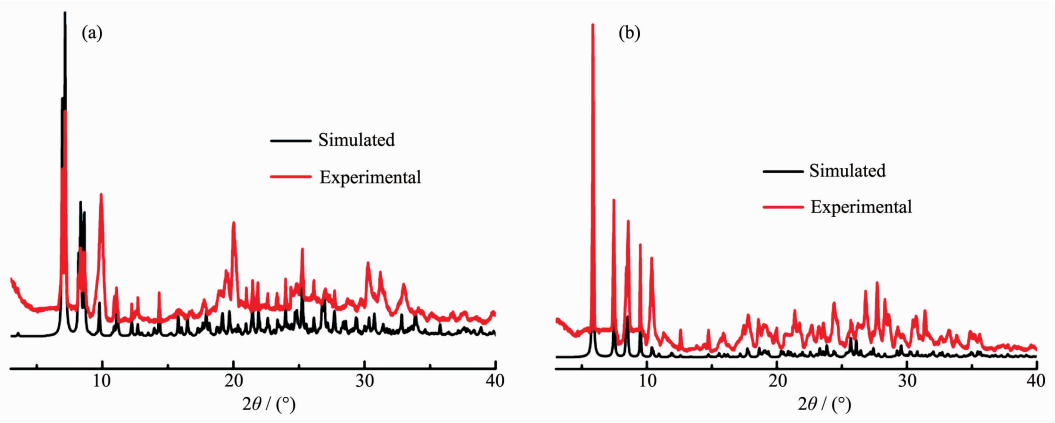

Fig.5　PXRD patterns of crystals **1** (a) and **2** (b)

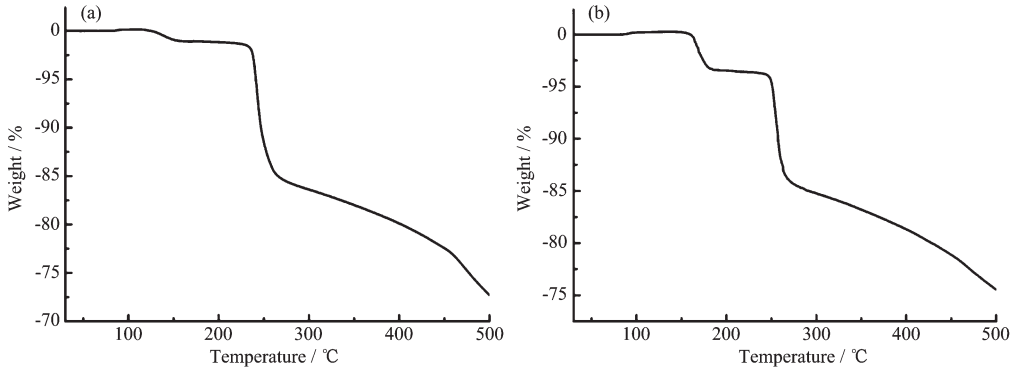

Fig.6　TG-DTA plots of crystals **1** (a) and **2** (b)

crystals **1** and **2**.

2.5　Diffuse reflectance spectra for crystals 1 and 2

UV-Vis spectra of the crystalline salts dispersed in barium sulfate was obtained by the diffuse reflectance technique[24]. Crystals **1** and **2** in the solid state showed a broad, upper-energy absorptions that extended from 300 nm to well beyond 800 nm. It can be observed that the absorption intensities from 420 to 800 nm of crystals **1** and **2** are much stronger than starting materials $[SMo_{12}O_{40}]^{2-}$ as shown in Fig.7. According to the Mulliken theory[24], these results can be attributed to charge-transfer transitions between the $[SMo_{12}O_{40}]^{2-}$ acceptor and supramolecular cationic donor.

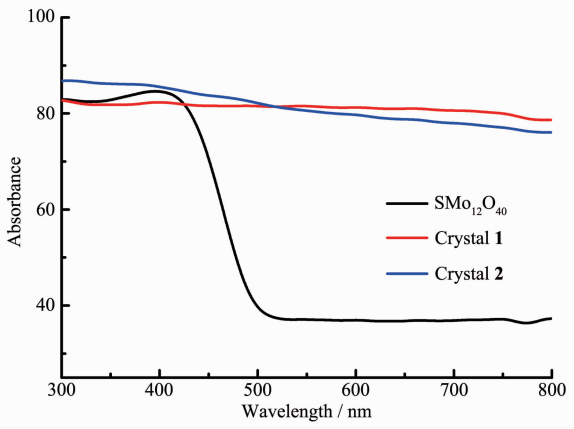

Fig.7　Diffuse reflectance spectra of $SMo_{12}O_{40}$, crystals **1** and **2**

3　Conclusions

Supramolecular structural inorganic-organic hybrids $[(4\text{-I-Anis})([18]\text{crown-6})]_2[SMo_{12}O_{40}]\cdot CH_3CN$ (**1**) and $[(3\text{-F-4-Cl-Anis})_2\ (DB[30]\text{crown-10})][SMo_{12}O_{40}]\cdot 2CH_3CN$ (**2**) have been synthesized based on the structural advantages of POMs and crown ethers. Crystals **1** and **2** are constructed through noncovalent bonding interaction. Supramolecular cation are formed through the N–H⋯O hydrogen bonding interaction between the nitrogen atom of anilinium and oxygen atoms of crown ether derivatives. In crystal **1**, small size monovalent supramolecular cations (4-I-Anis)([18]crown-6) was designed, and each polyoxoanion is surrounded by six monovalent supramolecular cations to form hexagonal arrangement in *bc* plane. In crystal

2, a larger size divalent supramolecular cations (3-F-4-Cl-Anis)$_2$(DB[30]crown-10) was chosen, and each polyoxoanion is surrounded by four divalent supramolecular cations to form tetragonal arrangement in the *bc* plane. TG results indicate that hydrogen bonding interaction plays an important role in maintaining the structural stability of crystals **1** and **2**. UV-Vis DRS spectra indicate that there exists charge-transfer interaction between $[SMo_{12}O_{40}]^{2-}$ and crown ether based supramolecular cations in crystals **1** and **2**.

Acknowledgements: The authors thank the Foundation of Wuhan Textile University (Grant No.165002), Hubei Natural Science Foundation (Grant No.2018CFB402), Hubei Key Laboratory of Biomass Fibers and Eco-dyeing & Finishing, and Hubei Key Laboratory for Processing and Application of Catalytic Materials (Grant No.201829203) for supporting this work.

References:

[1] Taleghani S, Mirzaei M, Eshtiagh-Hosseini H, et al. *Coord. Chem. Rev.*, **2016**,**309**:84-106

[2] XIONG Jun(熊俊), LI Ming(李明), YANG Shui-Bin(杨水彬), et al. *Chinese J. Inorg. Chem.*(无机化学学报), **2017**,**33**:1649-1655

[3] Moulton B, Zaworotko M F. *Chem. Rev.*, **2001**,**101**:1629-1658

[4] Evans O R, Lin W. *Acc. Chem. Res.*, **2002**,**35**:511-522

[5] Tayi A S, Kaeser A, Aida T, et al. *Nat. Chem.*, **2015**,**7**:281-294

[6] Mukherjee A, Tothadi S, Desiraju G R. *Acc. Chem. Res.*, **2014**,**47**:2514-2524

[7] Mirzaei M, Eshtiagh-Hosseini H, Alipour M, et al. *Coord. Chem. Rev.*, 2014,275:1-18

[8] von Allmen K, Moré R, Müller R, et al. *ChemPlusChem*, **2015**,**80**:1389-1398

[9] Ibrahim M, Mereacre V, Leblanc N, et al. *Angew. Chem. Int. Ed.*, **2015**,**54**:15574-15578

[10]Folkman S J, Finke R G. *ACS Catal.*, **2017**,**7**:7-16

[11]YAN Jing-Sen(鄢景森), AI Li-Mei(艾丽梅), WANG Qiang(王强), et al. *Chinese J. Inorg. Chem.*(无机化学学报), **2018**,**34**:2179-2187

[12]Long D L, Burkholder E, Cronin L. *Chem. Soc. Rev.*, **2007**,**36**:105-121

[13]Akutagawa T, Kudo F, Tsunashima R, et al. *Inorg. Chem.*, **2011**,**50**:6711-6718

[14]Niu Y J, Ren X Y, Yin B, et al. *J. Organomet. Chem.*, **2010**,**695**:1863-1868

[15]Nishihara S, Akutagawa T, Nakamura T, et al. *Chem. Asian J.*, **2007**,**2**:1083-1090

[16]Akutagawa T, Endo D, Nakamura T, et al. *Coord. Chem. Rev.*, **2007**,**251**:2547-2561

[17]Xiong J, Kubo K, Nakamura T, et al. *Cryst. Growth Des.*, **2016**,**16**:800-807

[18]Xiong J, Kubo K, Nakamura T, et al. *CrystEngComm*, **2015**,**17**:856-861

[19]Sanchez C, Livage J, Launay J P, et al. *J. Am. Chem. Soc.*, **1982**,**104**:3194-3202

[20]Sheldrick G M. *SHELXS*-97, *Program for the Solution of Crystal Structures*, University of Göttingen, Germany, **1997**.

[21]Sheldrick G M. *SHELXL*-97, *Program for the Refinement of Crystal Structures*, University of Göttingen, Germany, **1997**.

[22]Steiner T. *Angew. Chem. Int. Ed.*, **2002**,**41**:48-76

[23]Rathore R, Lindeman S V, Kochi J K. *J. Am. Chem. Soc.*, **1997**,**119**:9393-9403

[24]Mulliken R S. *J. Am. Chem. Soc.*, **1950**,**72**:600-608